MECHANICAL AND FRACTURE PROPERTIES OF EPOXY SYNTACTIC FOAMS MODIFIED WITH MILLED CARBON FIBRE

Sammy He[1], Declan Carolan[1,2], Alexander Fergusson[1,2] and Ambrose C. Taylor[1]

[1] Department of Mechanical Engineering, Imperial College London, London SW7 2AZ, UK
Email: sammy.he12@imperial.ac.uk (S. He), a.c.taylor@imperial.ac.uk (A. C. Taylor)
Webpage: http://www.imperial.ac.uk/people/a.c.taylor (A. C. Taylor)

[2] FAC Technology, 53 Lydden Grove, Wandsworth, London SW16 4LW, UK
Email: declan@factechnology.com (D. Carolan), alex@factechnology.com (A. Fergusson)

Keywords: syntactic foam, epoxy matrix composite, hollow glass microspheres, milled carbon fibre, tension, fracture, toughening mechanisms

Abstract
Syntactic foams are lightweight but brittle materials typically used as the core for sandwich composite panels. Foams comprising of ∼60 vol% hollow glass microspheres (GMS) in an epoxy matrix were modified by the addition of milled carbon fibre (MCF). Weight ratios of up to 30% MCF:GMS were used. The tensile modulus of the foams increased from 3.36 GPa up to 4.82 GPa with the addition of 30% weight ratio of MCF. The tensile failure strength of the syntactic foam decreased with low loadings of MCF, which is attributed to low load transfer capacity among the fibres due to poor fibre population. The tensile failure strength recovers when more MCF particles are added. The fracture energy of the syntactic foam showed an increase of 217%, from 182 J/m^2 to 396 J/m^2, due to the addition of 30% weight ratio of MCF. Toughening mechanisms were identified as crack deflection, debonding and subsequent plastic void growth, and fibre pull-out.

1. Introduction

Syntactic foams are composite materials comprising of hollow particles in a matrix material. The present work prepared densely packed syntactic foams using hollow glass microspheres (GMS) in a thermosetting polymer matrix. These materials exhibit desirable properties such as low density, high specific strength, high compressive strength, low moisture absorption, and low thermal and electrical conductivity, making them attractive for structural, weight-sensitive applications in aerospace and marine industries, such as the core in sandwich composites [1]. However, the uses of syntactic foams are limited due to their brittle nature. One method to improve their fracture toughness is to reduce the GMS volume fraction in the syntactic foam, at a cost of increasing the density [2]. Alternative attempts to improve the mechanical and fracture properties include the addition of particles such as nanoclay [3], crumb rubber [4], and various high aspect ratio fibres [5, 6]. However, processability becomes increasingly difficult at high particle loadings. Studies of fibre-reinforced syntactic foams with densely-packed GMS are therefore relatively rare.

This study investigates the effect of milled carbon fibre (MCF) particles on the tensile and fracture properties of a syntactic foam. The volume fraction of the particles is kept constant for all of the syntactic foam formulations at around 60% to minimise density. The tensile modulus, tensile strength, fracture

toughness and fracture energy are measured. The toughening mechanisms are then identified using scanning electron microscopy.

2. Experimental

2.1. Materials and manufacturing

The matrix for the syntactic foams is an anhydride-cured epoxy. The epoxy resin was a standard diglycidyl ether of bisphenol-A (DGEBA), 'Araldite LY556', with an epoxide equivalent weight (EEW) of 185 g/eq. This was cured using a methyltetrahydrophtalic anhydride, 'Aradur HY917', with an anhydride equivalent weight (AEW) of 166 g/eq. The curing process was accelerated by a heterocyclic amine catalyst, 1-methylimidazole, 'Accelerator DY070'. All epoxy components were supplied by Huntsman, UK. A stoichiometric ratio of 90 parts per hundred resin (phr) of HY917 and 1 phr of DY070 was used.

Borosilicate glass microspheres of type 'S38' from 3M, UK, were used to manufacture the syntactic foams. These microspheres have a mean diameter of 40 μm, and a true density of 380 kg/m^3 [7]. Milled carbon fibres were used as the modifier, supplied as 'Carbiso Mil 100μ' from easycomposites, UK. The MCF have a mean length of 100 μm and a mean diameter of 7.5 μm, with a true density of 1800 kg/m^3 [8]. The MCF was added at weight ratios up to 30% MCF:GMS. The required amounts of MCF and GMS were manually mixed until a uniform grey-coloured powder was achieved. This was passed through a sieve with holes approximately 1.5 mm square several times to remove agglomerations of MCF.

The particles are randomly close packed so that the particle volume fraction of the syntactic foams is around 60%. The syntactic foams were made using FAC Technology's manufacturing process. The epoxy matrix was prepared by mixing LY556 with HY917 and DY070, followed by a degassing in a vacuum. The syntactic foam was cured at 80 °C for 4 hours, followed by a post-cure at 140 °C for 8 hours as recommended by Huntsman.

2.2. Mechanical testing

The tensile properties of the syntactic foam was determined by uniaxial tensile tests in accordance with the ISO 527-1 [9] test standard. At least five specimens of type 1BA were tested at a loading rate of 1 mm/min, with the strain being measured using a clip-on extensometer. The tensile modulus was calculated over the strain interval of 0.0005-0.0025.

The fracture toughness, K_{IC}, and fracture energy, G_{IC}, were determined using single edge notch bending (SENB) tests in accordance with the ISO 13586 [10] test standard. Specimens of dimensions 80 $\times$ 16 $\times$ 8 mm^3 were tested at a displacement rate of 1 mm/min. A liquid nitrogen cooled razor blade was carefully tapped into a machined V-notch to produce a sharp pre-crack before testing. At least five valid tests were performed for each syntactic foam formulation.

2.3. Image analysis

A Hitachi S-3400N scanning electron microscope (SEM) was used to observe the fracture surfaces of the SENB samples to identify the toughening mechanisms. The samples were sputter-coated with a 10 nm thick layer of chromium to minimise charging. An accelerating voltage of 10 kV was used.

Optical microscopy was used to observe the microstructure of the syntactic foams. Cross-sections of

the samples were cold-mounted using an acrylic resin (VARI-SET 10), and were subsequently ground and polished to a 0.25 µm finish using a Saphir 330 polishing machine. The optical micrographs were obtained using an AxioScope.A1 optical microscope.

3. Results & Discussion

3.1. Microstructure

The microstructure of the syntactic foams was determined by the micrographs from optical and SEM mimcroscopy. The micrographs show that the glass microspheres are densely packed within the epoxy matrix. Individual carbon fibres can be seen in the SEM images, or as bright spots in the optical microscopy images due to their reflective nature. The images show that the fibres are in a 3D random orientation. Defects such as matrix voids and agglomerations of MCF particles were also present, see Figure 1.

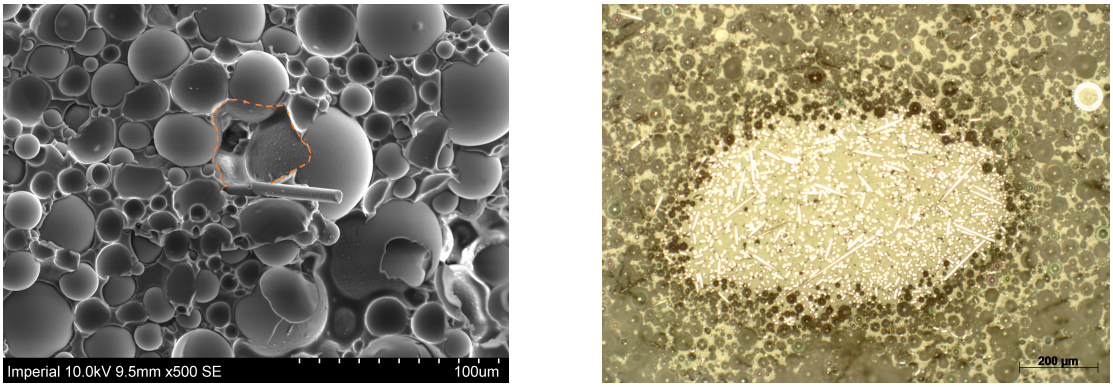

(a) **(b)**

Figure 1: (a) SEM image of a void (outlined in dashed orange) entrapped by a carbon fibre and (b) optical microscopy image of an agglomeration of MCF particles

3.2. Tension

Tensile tests were conducted on the syntactic foam formulations. The measured tensile modulus, E_t, and tensile failure true strength, σ_t, of the samples are shown in Figure 2.

The tensile modulus increases with higher MCF ratios, which is expected due to the high modulus of the carbon fibre (200 GPa [8]) compared to the unmodified syntactic foam (3.36 GPa). This increase can be predicted using the Halpin-Tsai model [11]:

$$E = \frac{1+\zeta\eta V_f}{1-\eta V_f} E_m \tag{1}$$

$$\eta = \frac{\frac{E_f}{E_m} - 1}{\frac{E_f}{E_m} + \zeta} \tag{2}$$

where E_m is the modulus of the matrix, E_f is the modulus of the particles, and V_f is the volume fraction

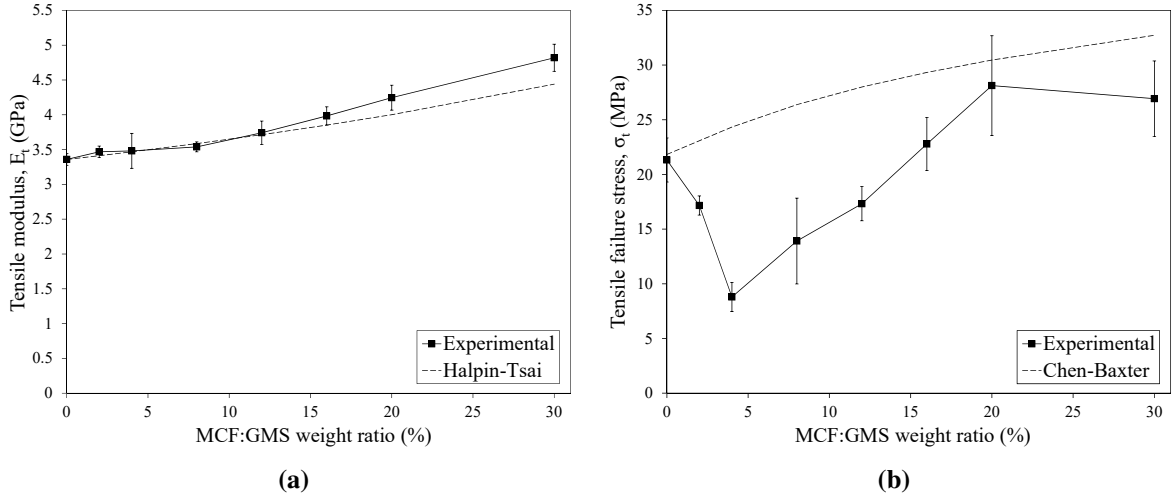

Figure 2: (a) Tensile modulus and (b) tensile failure strength of MCF modified syntactic foams.

of the particles. The geometry factor, ζ, depends on the particle orientation. For particles aligned in the loading direction, $\zeta = 2\,(l/t)$, where l and t are the length and thickness of the particle respectively. This will give the modulus in the loading direction, E_{11}. For particles aligned in the perpendicular direction, $\zeta = 2$, giving the perpendicular modulus, E_{22}. For rod-like particles arranged in a random orientation, van Es [12] showed that the modulus has a contribution from both components:

$$E = 0.184\,E_{11} + 0.816\,E_{22} \tag{3}$$

Comparison of the Halpin-Tsai model to the experimental results showed close agreement, as shown in Figure 2a.

A drop in tensile failure strength was observed in syntactic foams modified with up to 4% weight ratio of MCF. The tensile failure strength then recovers when the weight ratio is further increased. Rojo et al. [13] observed similar behaviour with cellulose fibre reinforced composites at low fibre loadings. They attributed the drop in tensile strength at low fibre loading to poor load transfer capacity between neighbouring fibres.

A number of other microstructural features were observed at all particle loadings. The small addition of fibres entrapped voids as shown in Figure 1a, which act as points of stress concentration in the syntactic foam, promoting material failure. Agglomeration of MCF particles was also evident, see Figure 1b. Insufficient wetting of MCF particles by the resin inside these fibrous agglomerations is likely as the resin cannot adequately penetrate the tightly packed structure. These agglomerations will act as additional stress concentrations, promoting early failure of the composite.

Once the tensile failure stress recovers, the stresses show reasonable agreement to the model developed by Baxter [14] for composites with randomly oriented discontinuous fibres. This model utilises the equations for the three failure mechanisms in fibre reinforced composites postulated by Jackson and Cratchley [15] and combines them in the Tsai-Hill failure criterion, giving:

$$\sigma_t = \frac{1}{\pi}\int_0^{\pi}\left[\frac{\cos^4\theta}{\sigma_L^2} + \left(\frac{1}{\tau^2} - \frac{1}{\sigma_L^2}\right)\sin^2\theta\cos^2\theta + \frac{\sin^4\theta}{\sigma_T^2}\right]^{-1/2} \mathrm{d}\theta \tag{4}$$

where θ is the angle between the fibre direction and the applied stress, σ_L is the longitudinal strength of the composite with aligned fibres, σ_T is the equivalent transverse strength, and τ is the interfacial strength between the matrix and fibre. The matrix in this context is the unmodified syntactic foam.

3.3. Fracture

The fracture toughness, K_{IC}, and the fracture energy, G_{IC}, of the MCF modified syntactic foams were determined using SENB tests, and are shown in Figure 3. Both K_{IC} and G_{IC} increase with increasing MCF content, with a fracture toughness of 1.38 MPa $m^{1/2}$ and a fracture energy of 396 J/m^2 being measured for syntactic foam modified with 30% weight ratio of MCF. This shows good promise for MCF as a toughener for syntactic foams.

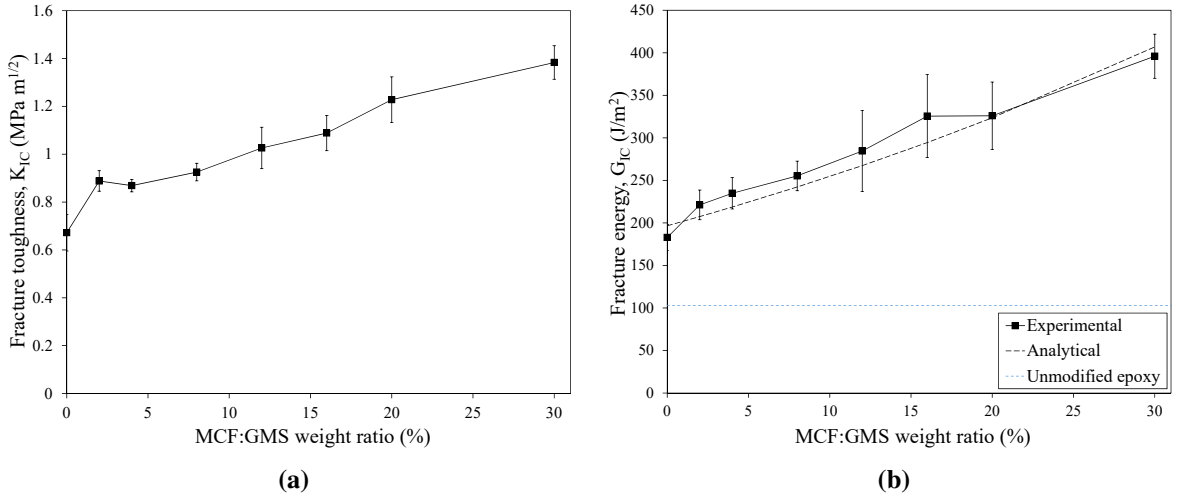

Figure 3: (a) Fracture toughness and (b) fracture energy of MCF modified syntactic foams.

3.4. Fractography

Scanning electron microscopy was used to examine the fracture surfaces in the vicinity of the pre-crack tip to determine the toughening mechanisms. Crack deflection is evident from the step structures in the epoxy and the characteristic 'tails' behind the rigid particles. Fibre fracture and pull-out are also evident from the exposed fibres and cavities left by the fibres on the fracture surface. Debonding and subsequent void growth can be seen for both GMS and MCF particles. The voids left by the GMS particles showed an average 8% increase in volume, while voids left by MCF showed an average 32% increase in volume. The different toughening mechanisms are shown in Figure 4.

3.5. Prediction of fracture energy

The fracture energy of the modified syntactic foam can be predicted analytically using:

$$G_{IC} = G_{ICU} + \Psi \tag{5}$$

where G_{ICU} is the fracture energy of the unmodified epoxy and Ψ is the fracture energy contributions from the toughening mechanisms provided by the particles. The unmodified epoxy had a fracture energy of 103 J/m^2.

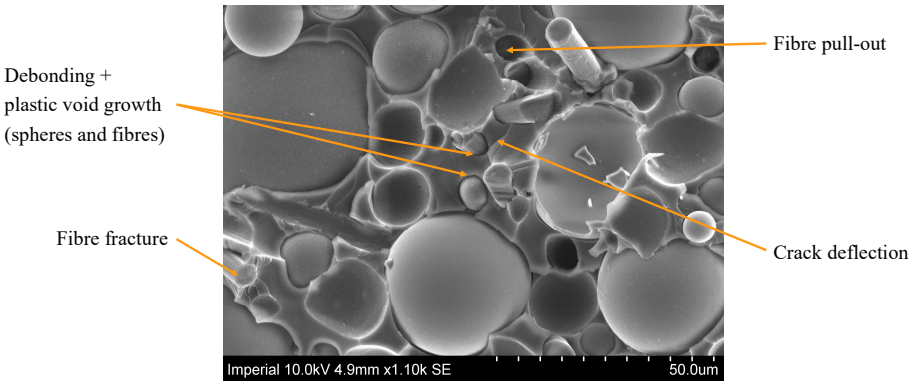

Figure 4: Toughening mechanisms of MCF modified syntactic foams

The fracture energy contribution from crack deflection, ΔG_{cd}, can be predicted using the Faber and Evans [16] model. This takes into account the tilt and twist of the crack front when it approaches a rigid particle. The deflected crack is subjected to local mixed-mode loading which increases the strain energy release rate, thus imparting an increase in fracture toughness.

Hull and Clyne [17] derived the expression to predict the fracture energy contribution from particle debonding, ΔG_{db}:

$$\Delta G_{db} = \int_0^L \frac{V_f}{\pi r^2 L} 2\pi r x_o G_{if} \, \mathrm{d}x_o \tag{6}$$

where x_o is the embedded length of the particle in the matrix, L is half the length of the particle, r is the radius of the particle and G_{if} is the interfacial fracture energy between the particle and the matrix. Integrating leads to the expressions for debonding energy for spheres and fibres respectively:

$$\Delta G_{db}^{GMS} = V_f^{GMS} \ln(4) G_{if}^{GMS} \tag{7}$$

$$\Delta G_{db}^{MCF} = \frac{V_f^{MCF} L}{r} G_{if}^{MCF} \tag{8}$$

The interfacial fracture energy for MCF in epoxy was determined experimentally by Wang et al. [18] and is taken as 10 J/m^2. For GMS, the interfacial fracture energy can be calculated using [19]:

$$G_{if}^{GMS} = \frac{3\sigma_{yt}^2 r}{4\pi E_m} \tag{9}$$

where σ_{yt} is the tensile yield stress of the matrix.

The fracture energy contribution from fibre pull-out, ΔG_{po}, was also derived from Hull and Clyne [17]:

$$\Delta G_{po} = \frac{V_f L^2}{3r} \tau_i \tag{10}$$

where τ_i is the interfacial shear strength for the particle/epoxy interface. For MCF, Wang et al. determined that $\tau_i = 28.12$ MPa [18]. This equation assumes unidirectional fibre alignment and perfect matrix-to-fibre

adhesion. Since the MCF particles are randomly orientated, the fracture energy contribution from particle pull-out will be overestimated. The effective fibre length, $\bar{l}$, for randomly oriented fibres can be calculated using [5]:

$$\bar{l} = \frac{\int_0^{\pi/2}\int_0^{\pi/2} l\cos\theta\cos\phi \; \mathrm{d}\theta\mathrm{d}\phi}{(\pi/2)^2} \tag{11}$$

where θ and ϕ are the angles projected on the loading axis and loading plane respectively. This gives an effective fibre length of $\bar{l} = 0.41l$, and this length is used in Equation 10.

The plastic void growth contribution to the fracture energy was calculated using [20]:

$$\Delta G_v = \left(1 - \frac{\mu_m^2}{3}\right)(V_{fv} - V_f)\,\sigma_{yc} r_{yu} K_{vm}^2 \tag{12}$$

where μ_m is the pressure dependent material constant which is taken as 0.2 [21], V_{fv} is the volume fraction of the voids, and σ_{yc} is the compressive yield strength of the unmodified epoxy. The radius of the plastic zone, r_{yu}, can be calculated using the equation proposed by Irwin [22]:

$$r_{yu} = \frac{1}{6\pi}\left(\frac{K_{CU}^2}{\sigma_{yt}^2}\right) \tag{13}$$

where K_{CU} is the fracture toughness of the unmodified epoxy. The von Mises stress concentration factor, K_{vm}, varies linearly with volume fraction of the particles [23]:

$$K_{vm} = 0.59V_f + 1.65 \tag{14}$$

When all of the above models are applied, the prediction in fracture energy shows good agreement with the experimental values, see Figure 3b. The fracture energy contribution from each of the toughening mechanisms is shown in Figure 5. The contribution from fibre pull-out becomes the dominant toughening mechanism at higher MCF weight ratios. The contributions from the other toughening mechanisms are approximately constant, as they depend on the particle volume fraction which remains at approximately 60%.

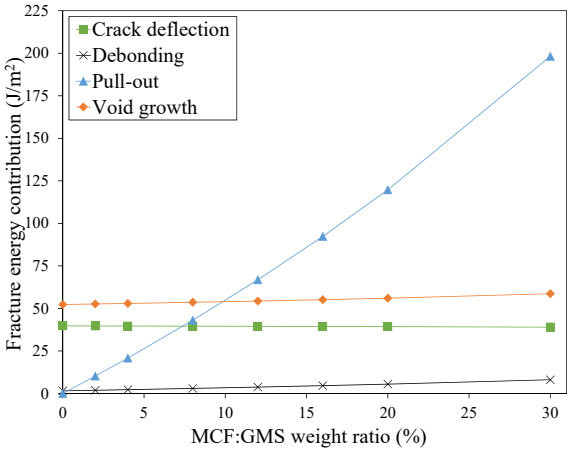

Figure 5: Fracture energy contributions from the identified toughening mechanisms

4. Conclusions

The tensile and fracture properties of syntactic foams reinforced with milled carbon fibre (MCF) were measured. Milled carbon fibre was added to the glass microspheres (GMS) at different weight ratios. At 30% weight ratio, the tensile modulus of the syntactic foam increased to 4.82 GPa from 3.36 GPa for the unmodified syntactic foam. The Halpin-Tsai model for tensile modulus shows good agreement to the experimental data. The fracture energy also increased to 396 J/m^2 at 30% MCF:GMS weight ratio from 183 J/m^2 for the unmodified, showing good promise for MCF as a toughener in syntactic foams. Scanning electron microscopy identified the toughening mechanisms as crack deflection, fibre pull-out, and debonding with subsequent plastic void growth. Analytical modelling of these toughening mechanisms showed good agreement to the experimental data, and showed that fibre pull-out is the main contributor to fracture toughness at higher loadings of MCF.

References

[1] N. Gupta, S. E. Zeltmann, V. C. Shunmugasamy, and D. Pinisetty. Applications of polymer matrix syntactic foams. *JOM*, 66(2):245–254, 2013.

[2] E. M. Wouterson, F. Y. C. Boey, X. Hu, and S. Wong. Specific properties and fracture toughness of syntactic foam: Effect of foam microstructures. *Composites Science and Technology*, 65(1112):1840–1850, 2005.

[3] R. R. Maharsia and H. D. Jerro. Enhancing tensile strength and toughness in syntactic foams through nanoclay reinforcement. *Materials Science and Engineering: A*, 454455:416–422, 2007.

[4] M. A. Wahab, V. B. Gorugantu, and N. Gupta. Enhancement of fracture toughenss of syntactic foams by rubber addition. In *Proceedings of the 2005 ASME International Mechanical Engineering Congress and Exposition (IMECE2005)*, pages 187–192, Orlando, Florida, USA, 2005.

[5] E. M. Wouterson, F. Y. C. Boey, X. Hu, and S. Wong. Effect of fiber reinforcement on the tensile, fracture and thermal properties of syntactic foam. *Polymer*, 48(11):3183–3191, 2007.

[6] J. A. M. Ferreira, C. Capela, and J. D. Costa. A study of the mechanical behaviour on fibre reinforced hollow microspheres hybrid composites. *Composites Part A: Applied Science and Manufacturing*, 41(3):345–352, 2010.

[7] 3M. *Technical data sheet of 3M Glass Bubbles S38*. 3M, USA, 2010.

[8] easycomposites. *Technical data sheet of Carbiso Milled Carbon Fibre*. easycomposites, UK, 2011.

[9] ISO 527-1. *Plastics - Determination of tensile properties - Part 1: General principles*. International Standards Organisation, Geneva, 1996.

[10] ISO 13586. *Plastics - Determination of fracture toughness (G_{IC} and K_{IC}) - Linear elastic fracture mechanics (LEFM) approach*. International Standards Organisation, Geneva, 2000.

[11] J. C. Halpin and J. L. Kardos. Halpin-Tsai equations: A review. *Polymer Engineering and Science*, 16(5):344–352, 1976.

[12] M. A. van Es. *Polymer-clay nanocomposites: The importance of particle dimensions*. PhD thesis, Faculty of Applied Sciences, Delft University of Technology, 2001.

[13] E. Rojo, M. V. Alonso, M. Oliet, B. D. Saz-Orozco, and F. Rodriguez. Effect of fibre loading on the properties of treated cellulose fibre-reinforced phenolic composites. *Composites Part B: Engineering*, 68:185–192, 2015.

[14] W. J. Baxter. The strength of metal matrix composites reinforced with randomly oriented discontinuous fibres. *Metallurgical Transactions A*, 23(11):3045–3053, 1992.

[15] P. W. Jackson and D. Cratchley. The effect of fibre orientation on the tensile strength of fibre-reinforced metals. *Journal of the Mechanics and Physics of Solids*, 14(1):49–64, 1966.

[16] K. T. Faber and A. G. Evans. Crack deflection processes - I. Theory. *Acta Metallurgica*, 31(4):565–576, 1983.

[17] D. Hull and T. W. Clyne. *An Introduction to Composite Materials*. Cambridge University Press, 2nd edition, 1996.

[18] C. Wang, X. Ji, A. Roy, V. V. Silberschmidt, and Z. Chen. Shear strength and fracture toughness of carbon fibre/epoxy interface: effect of surface treatment. *Materials & Design*, 85:800–807, 2015.

[19] A. N. Gent. Detachment of an elastic matrix from a rigid spherical inclusion. *Journal of Materials Science*, 15(11):2884–2888, 1980.

[20] Y. Huang and A. J. Kinloch. Modelling of the toughening mechanisms in rubber-modified epoxy polymers - Part II A quantitative description of the microstructure-fracture property relationships. *Journal of Materials Science*, 27(10):2763–2769, 1992.

[21] J. N. Sultan and F. J. McGarry. Effect of rubber particle size on deformation mechanisms in glassy epoxy. *Fatigue and Fracture of Engineering Materials and Structures*, 13(1):29–34, 1973.

[22] G. R. Irwin. Plastic zone near a crack and fracture toughness. In *Meeting of the 7th Sagamore Ordnance Materials Research Conference*, pages 63–78, Racquette Lake, New York, USA, 1960.

[23] F. J. Guild and R. J. Young. A predictive model for particulate-filled composite materials - Part 1 Hard particles. *Journal of Materials Science*, 24(1):298–306, 1989.